IMPACT DELIVERY OF WATER AT THE MOON AND MERCURY. M. Bruck Syal[1] and P. H. Schultz[2], [1]Lawrence Livermore National Laboratory, Livermore, CA 94551 (syal1@llnl.gov) [2]Brown University, Providence, RI 02912

Introduction: Cometary and asteroidal impacts at Mercury and the Moon supply some fraction of these bodies' near-surface reservoirs of water ice. At Mercury, MESSENGER spacecraft observations of permanently shadowed regions reveal bright and dark deposits, interpreted as comet- or asteroid-derived water and organics [1]. At the Moon, excavation of a permanently shadowed crater by the LCROSS mission confirmed the presence of substantial (~5 wt%) near-surface water [2]. Here we calculate the total mass of water delivered by impacts to the Moon and Mercury, determine the primary water sources for each body, and compare these results with observational constraints.

We present new insights on delivery efficiency from simulations using the CTH shock physics code [3]. Integrating these results with current estimates for comet, asteroid, and micrometeorite fluxes at the Moon and Mercury provides a more complete understanding of exogenous water sources. While prior analytical and numerical work has treated aspects of this problem [4,5], the effects of parameters such as impact angle, porosity, and impactor composition have not yet been characterized in detail. This study is the first to directly compare impact delivery of water at these bodies.

Numerical Approach: A mass-filtering algorithm tracks the impactor mass remaining below escape speed for the Moon (v_{esc}=2.38 km/s) and Mercury (v_{esc}=4.25 km/s). This method compares well to tracer particle-based approaches, with the benefit of improved resolution. Table 1 summarizes the range of initial conditions simulated and material models employed for asteroidal and cometary impacts.

Table 1: Computational Parameters: Comet & Asteroid Impacts

Parameter	Value
$D_{projectile}$	1 km
v_{impact}	15.0 - 60.0 km/s
θ (impact angle)	15° - 90°
Comet EOS[a]	ANEOS Water Ice
Asteroid EOS	ANEOS Mg_2SiO_4
Target regolith EOS	ANEOS SiO_2
ϕ (porosity: impactors and target)	0.0 - 0.6
P-α crush strength H_2O	0.1 GPa
P-α crush strength SiO_2	1.0 GPa
2D resolution	36 cppr[b]
3D resolution	18 cppr
Mercury v_{escape}	4.25 km/s
Moon v_{escape}	2.38 km/s

[a]Equation of State
[b]cells-per-projectile-radius

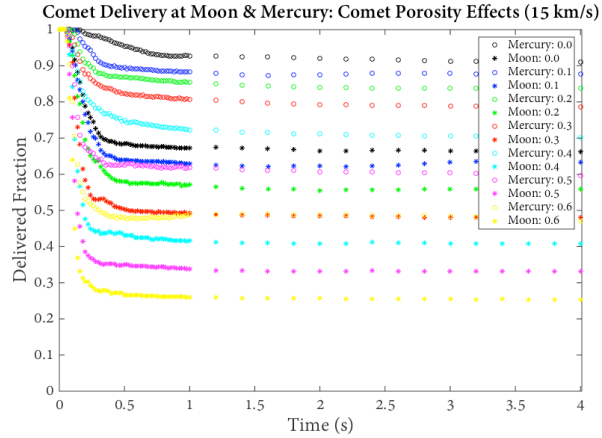

Fig. 1. Example time dependence of delivered fraction of impactor material (here, for a range of porosities). Note that the answer converges within the first few seconds, as vapor plume expansion becomes isentropic.

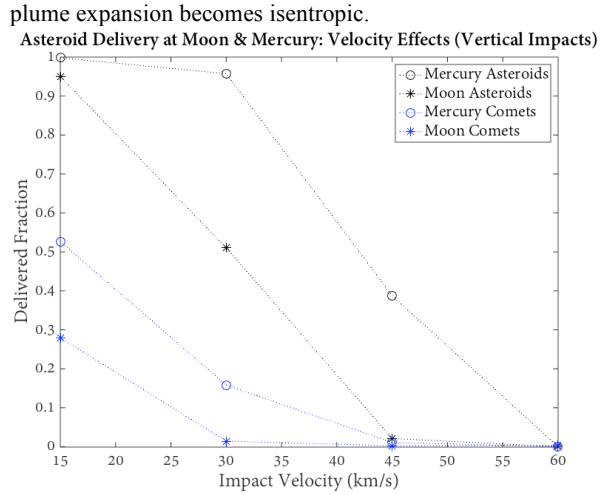

Fig. 2. Fraction of impactor retained depends upon the internal energy of the vapor plume, which scales as ~v^2. Previous work investigated this relationship for cometary bodies at the Moon [5]. We extend calculations to Mercury and also to asteroidal bodies, which are retained more efficiently, due to differing impedance matching conditions and higher specific energies of vaporization.

Results: Impact retention depends upon velocity, impact angle, and material properties (Fig. 1-4). These composite effects are calculated for the Moon and Mercury using Eqn. (1), assuming asteroid and micrometeorite densities of 2.0 gcm^{-3}, comet densities of 0.5 gcm^{-3}, and target regolith densities of 2.55 gcm^{-3}.

We find that asteroids deliver the bulk (>95%) of water to the Moon (1.00×10^{16} kg Gyr^{-1}), while micrometeorites (>90% cometary in origin) [6,7] provide most (>99%) of Mercury's delivered water (1.17×10^{16} kg Gyr^{-1}). Cometary delivery rates are relatively low, due to their higher median impact speeds, less

efficient retention than stony impactors at equivalent speeds (Fig. 2), and lower fluxes (relative to micrometeorites and asteroids).

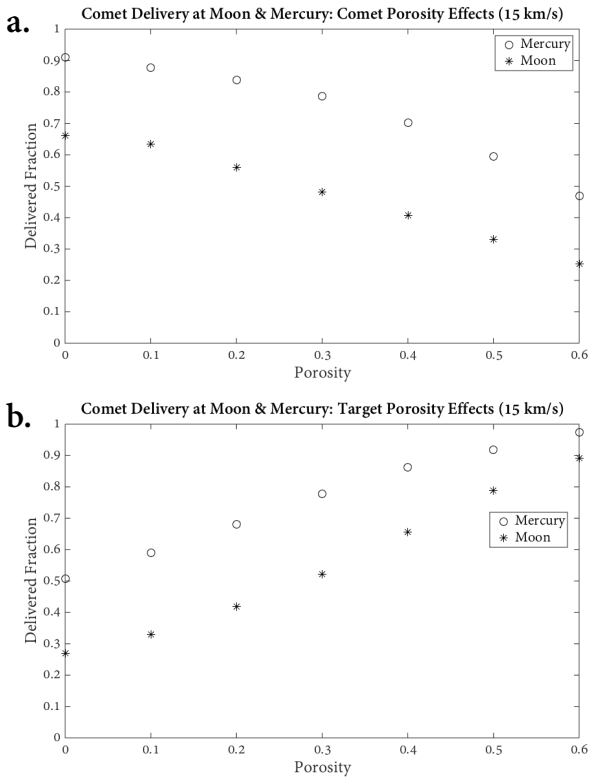

Fig. 3. Impactor porosity (**a.**) contributes to decreased retention (through additional heating of impactor material from pore compaction, along with enhanced energy partitioning to the impactor), while target porosity (**b.**) promotes enhanced retention through decreased energy partitioning to the impactor and an elongated penetration cavity at early times [8]. Impactor porosity is important for most asteroids and comets; simulations in this study used significant porosity for each to match observational constraints. Target porosity may be especially important for micrometeorite impacts.

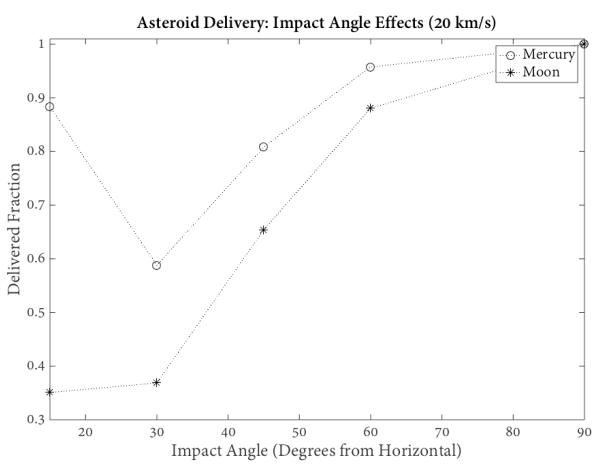

Fig. 4. Impact angle affects retention through different energy partitioning mechanisms [9] and peak pressure effects [10]. Increased energy partitioning to the impactor, relative to the target, results in decreased retention from 90° to 30°. At 15°, this effect is counteracted by decreasing peak pressures (which vary as $\sin^2\theta$).

Total fraction of impactor retained can be expressed as:

$$F = \int_{v_{min}}^{v_{max}} \int_0^{\pi/2} P(v) f(v) \sin(2\theta) f(\theta)\, d\theta\, dv \qquad (1)$$

where $P(v)$ is impact velocity probability distribution, $f(v)$ is fraction retained as a function of velocity, θ is impact angle, and $f(\theta)$ is fraction retained as a function of impact angle

Implications for H_2O at the Moon and Mercury: Impacts can deliver all near-surface water detected at the Moon and Mercury, without invoking separate mechanisms, over relatively short timescales. Accounting for migration to cold traps (20-50% survival) [11] and stability against space weathering (6% survival over 1 Gyr) [12], we conservatively assume that 1% of delivered water survives migration and subsequent bombardment.

At these rates, the estimated lunar H_2O reservoir (2×10^{12} kg) [13] is replenished over just 20 Myr and Mercury's estimated H_2O reservoir (4×10^{13} kg) [4] is replenished over 400 Myr. Differing impact-derived water sources for Mercury and the Moon may affect the time-dependency of both reservoirs. While the Moon receives most impact-delivered water in larger, episodic impacts (asteroids), Mercurian water should exhibit less variability over time, as water replenishment by micrometeorites is a relatively steady-state process. The episodic nature of water delivery on the Moon could explain the vertical structure of ices at the poles [14].

References:

[1] Neumann, G. et al. 2013. Science 339, 296-300. [2] Colaprete, A. et al. 2010. Science 330:463-468. [3] McGlaun, J.M. et al. 1990. Int. J. Impact Eng., 10:351-360. [4] Moses, J. et al. 1999. Icarus 137, 197–221. [5] Ong, L. et al. 2010. Icarus 207, 578–589. [6] Wiegert, P. et al. 2009. Icarus 201, 295–310. [7] Nesvorný, D. et al. 2010. Astrophys. J. 713, 816–836. [8] Schultz, P. & Eberhardy, C. 2014. Icarus (In Press). [9] Schultz, P. 1996. JGR 101:21,117–21,136. [10] Vickery, A.M., Melosh, H.J., 1990. Geol. Soc. of Am. (Special Paper), 289–300. [11] Butler, B.J., 1997. JGR 102, 19283–19291. [12] Crider, D.H., Vondrak, R.R., 2000. JGR. 105, 26773–26783. [13] Feldman, W.C. et al. 2000. JGR 105, 4175–4195. [14] Schultz, P. et al. (2010), Science 330, 463 – 468.

This work was performed under the auspices of the U.S. Department of Energy by Lawrence Livermore National Laboratory under Contract DE-AC52-07NA27344. LLNL-ABS- 665818